TRANSACTIONS OF THE INSTITUTE OF FLUID-FLOW MACHINERY

No. 139, 2018, 3–22

Thangavelu Kannan[a*], Arthanaari Malleswaran[a] and M.B.K. Moorthy

Effects of variable viscosity on natural convection flow of an optically thick gray gas past a horizontal surface in the presence of internal heat generation

[a] *Department of Mathematics, School of Arts, Science and Humanities, Sastra Deemed University, Thanjavur, Tamil Nadu-613401, India.*

[b] *Department of Mathematics, Thiruvalluvar Government Arts College, Rasipuram, Tamil Nadu- 631401, India*

Abstract

A numerical investigation to discuss the effects of radiation and variable viscosity on heat and mass transfer characteristics of natural convection over a horizontal surface embedded in a saturated porous medium in the presence of internal heat generation is carried out in this study. The working fluid for the investigation is optically thick gray gas. The Dufour and Soret effects are also taken into account. Similarity transformations are employed to obtain nonlinear ordinary differential equations from the governing equations of the present problem. The numerical results for the transformed governing equations are computed by using commercial boundary value problem solver for ordinary differential equations. The effects are discussed by varying the parameters such as radiation, Dufour and Soret numbers, buoyancy ratio, Prandtl number, Schmidt number, and variable viscosity. Presence of internal heat generation enhances the velocity profile and significantly decreases the concentration boundary layer thickness. On increasing fluid radiation, the temperature of the fluid is higher than that of the surface and the concentration boundary layer thickness decreases away from the surface.

Keywords: assisting and opposing flows, Dufour and Soret effects, internal heat generation, natural convection, radiation, variable viscosity.

*Corresponding author. E-mail adress: tkannanmat@gmail.com

Nomenclature

g	–	gravitational acceleration, m/s^2
f	–	dimensionless stream function
p	–	pressure, Pa
Ra_x	–	Rayleigh number
N	–	Buoyancy ratio
C	–	concentration, kg/m^2
C_∞	–	concentration at the free stream
C_w	–	concentration at the wall
C_s	–	concentration susceptibility
c_p	–	specific heat at constant pressure, J/kg K
x, y	–	Cartesian coordinates, m
Du	–	Dufour number
q_w	–	internal heat generation, W/m^3
Le	–	Lewis number
Nu_x	–	local Nusselt number
Sh_x	–	local Sherwood number
D_m	–	mass diffusivity
k_e	–	mean absorption coefficient
k	–	permeability, m^2
k_T	–	thermal diffusion ratio
Pr	–	Prandtl number
R	–	radiation parameter
q_r	–	radiative heat flux, W/m^2
Sc	–	Schmidt number
Sr	–	Soret number
T	–	temperature, K
T_∞	–	temperature of the uniform flow, K
k_T	–	thermal diffusion ratio, W/m K
u, v	–	velocity components, m/s
T_w	–	wall temperature, K

Greek symbols

α	–	thermal diffusivity, m^2/s
β	–	coefficient of thermal expansion, 1/K
β^*	–	concentration expansion coefficient
δ	–	constant defined in equation
η	–	dimensionless similarity variable
θ	–	dimensionless temperature
θ_c	–	variable viscosity parameter, kg/m s
μ	–	dynaqmic viscosity, kg/m s
μ_∞	–	free stream viscosity
υ	–	kinematic viscosity, m^2/s
ρ	–	fluid density, kg/m^3
σ_s	–	Stefan-Boltzmann constant, W/m^2K^4

φ – dimensionless concentration
ψ – stream function, m^2/s

Subscripts and superscript

w – condition at the wall
∞ – condition at the ambient medium
$'$ – differentiation with respect to η

1 Introduction

The study of heat and mass transfer by natural convection in a fluid saturated porous medium has acquired a great attention due to its significant role playing in many geophysical and engineering applications, atmospheric pollution control, energy-storage units, oil extraction, and ground water pollution. A detailed discussion of natural convection in porous medium can be found in the monographs by Ingham and Pop [1], Nield and Bejan [2], and Vafai [3]. Cheng and Minkowycz studied the effect of free convection past a vertical plate embedded in a porous medium with the application to heat transfer from a dike [4]. Lai and Kulacki carried out an investigation on the coupled heat and mass transfer by natural convection from vertical surface in a porous medium [5]. Mehrizi *et al.* presented an analysis of natural convection boundary layer flow on a horizontal plate with variable wall temperature in a new dimension [6]. Slawomir Henclik [7] proposed a mathematical model of flows with fluid-structure interaction.

As far as the heat and mass transfer processes are concerned, the mass transfer caused by the temperature gradient is referred to as the Soret or thermal-diffusion effect whereas the heat transfer caused by the concentration gradient is called Dufour or diffusion-thermo effect. When compared with the effects prescribed by Fourier's or Fick's laws, the thermal-diffusion and the diffusion-thermo effects are of smaller order magnitude and are often neglected in heat and mass transfer processes. Eckert and Drake proved that those effects cannot be neglected for some exceptional cases [8]. For example, the Soret effect has been used for isotope separation and in mixtures between gases with very light molecular weight (H_2, He). Further, the Dufour effect is found to have a remarkable magnitude for medium molecular weight (N_2, air). Badur *et al.* [9] investigaetd on Navier-Stokes boundary conditions in fluid mechanics and proposed the new, more general Navier-Stokes slip boundary condition. Anghel *et al.* investigated on thermal-diffusion (Soret) and diffusion-thermo (Dufour) effects [10]. They found that these effects appreciably influence the flow field in a free convection

boundary-layer over a vertical surface embedded in a porous medium. Lakshmi Narayana and Murthy discussed the Soret and Dufour effects on free convection heat and mass transfer from a horizontal flat plate in a Darcy porous medium [11]. El-Arabawy analyzed that the thickness of the thermal and concentration boundary layers increases notably when thermally opposing flow is considered [12]. Tai and Char concluded that the local Nusselt number increases with an increase in the Soret number or a decrease in the radiation parameter and the Dufour number [13]. Since the presence of internal heat generation affects the flow field, temperature and concentration distributions, consideration of internal heat generation in a problem is noteworthy. Some of the engineering applications involving internal heat generation are related in the fields of disposal of nuclear waste, storage of radioactive materials, nuclear reactor safety analyses, fire and combustion studies and in many industrial processes. Heat generation can be assumed to be constant, space dependent or temperature dependent. Crepeau and Clarksean considered a space dependent heat generation in their study on flow and heat transfer from vertical plate [14]. They proved that the exponentially decaying heat generation model can be used in mixtures where a radioactive material is surrounded by inert alloys. Similarity solutions of free convection boundary layers over vertical and horizontal surfaces in porous media with internal heat generation were reported by Postelnicu and Pop [15]. They found that the heat transfer is high when the internal heat generation is present. Alam *et al.* numerically studied the combined free-forced convection and mass transfer flow past a vertical porous plate in a porous medium with heat generation and thermal diffusion [16]. Sharma investigated the effects of viscosity and thermal conductivity on magnetohydrodynamics (MHD) steady free convective flow of a fluid along an isothermal plate in the presence of internal heat generation [17]. Makinde analyzed similarity solution for natural convection from a moving vertical plate with internal heat generation and a convective boundary condition [18]. Radiative heat transfer of an optically thick gray gas has its wide-spread applications in physics and engineering including space technology and other high-temperature processes such as propulsion systems, and plasma physics. Thermal radiation effect is essential to control heat transfer in manufacturing processes when the quality of the final product depends on heat control factors. High temperature plasmas, the cooling of nuclear reactors, liquid metal fluids, and power generation systems are some important applications of radiative heat transfer from a vertical wall to conductive gray fluids. In high-temperature chemical operations such as combustion and fire science, simulation of thermal radiation heat transfer will play a vital role in combination with conduction, convection, and mass transfer.

The convection-radiation heat transfer problems for an absorbing-emitting fluid along a vertical plate in a porous medium was analyzed by Raptis [19]. Hossain and Takhar investigated thermal radiation effects on natural convection flow over an isothermal horizontal plate [20]. They concluded that both the momentum and the thermal boundary layer thicknesses increase with an increase in both the radiation-conduction interaction and the surface temperature. Hossain *et al.l* [21] examined the effect of radiation on free convection flow of fluid with variable viscosity from a porous vertical plate. The effect of thermal radiation in the linearized Rosseland approximation on the heat transfer characteristics of various boundary layer flows was discussed by Magyari and Pantokratoras [22]. Siddiqaa *et al.* explicated the effect of thermal radiation on the natural convection boundary layer flow over a wavy horizontal surface [23]. It was shown that the heat transfer rate for the irregular horizontal surface is greater than that of the purely horizontal surface. Rup and Dróżdż computed the effect of reduced heat transfer in a micropolar fluid in natural convection [24]. Roszko and Fornalik-Wajs [25] analysed the heat transfer and flow structure in a strong magnetic field.

The viscous fluid flow involving temperature dependent properties has been dealt mostly in the literature since it has many powerful practical applications such as polymer processing industries, food processing, biochemical industries and enhanced recovery of petroleum resources. The viscosity of the fluids used in industries like polymer fluids, fossil fuels, etc. varies rapidly with temperature. As a result, variable viscosity of the fluid provides a physical interest instead of considering a constant viscosity. Lai and Kulacki analyzed the effect of variable viscosity on convective heat transfer along a vertical surface in a saturated porous medium [26]. They found that a significant error in the heat transfer coefficient occurs if the variable viscosity is neglected. Kumari made an analysis on variable viscosity effects on free and mixed convection boundary layer flow from a horizontal surface in a saturated porous medium-variable heat flux [27]. It was obtained that the heat transfer is bigger in the case of liquids when the variable viscosity is considered as compared to the constant viscosity case. When gases are under investigation, the heat transfer for variable viscosity is smaller than that of the constant viscosity. Kannan and Moorthy [28] numerically analsed the effects of variable viscosity on power-law fluids over a permeable moving surface with slip velocity in the presence of heat generation. Makinde discussed the effect of variable viscosity on thermal boundary layer over a permeable flat plate with radiation [29]. He made a conclusion that the local Nusselt number increases with a decrease in fluid viscosity. Cieśliński *et al.* reported the measurement of temperature-dependent viscosity and thermal conductivity in different working

fluids [30].

The above cited papers explicate the effects on free convection flow and the heat and mass transfer characteristics in horizontal plate embedded in porous medium with or without radiative heat transfer, Dufour and Soret effects and variable viscosity in detail. Obviously, presence or absence of internal heat generation becomes significant in many research works as explained above. It can be noticed that consideration of gases as working fluid in the place of liquids is of greater interest in practical applications in science and engineering. As a trial attempt, the authors intend to provide the knowledge of the effects of radiation, variable viscosity, Dufour and Soret effects with heat and mass transfer over a horizontal surface embedded in a porous medium filled with a optically thick gray gas in the presence of internal heat generation.

2 Mathematical analysis

Consider the steady, two-dimensional, viscous, incompressible boundary layer flow past a horizontal flat plate embedded in a porous medium in the presence of internal heat generation. The flow of the fluid is assumed to be an optically thick gray gas with the decisive importance to free convection, mass transfer and radiation. The physical model and the coordinate system are shown in Fig. 1. The Dufour and Soret effects are included for the present analysis. The properties of the fluid are constant except for the fluid density in the momentum equation. The porous medium is isotropic and homogeneous. The Boussinesq approximation for density and the boundary layer approximations are valid.

Under these assumptions, the governing equations of continuity, momentum, energy and concentration are written as follows:

$$\frac{\partial u}{\partial x} + \frac{\partial u}{\partial y} = 0 \,, \tag{1}$$

$$u = -\frac{k}{\mu}\left(\frac{\partial p}{\partial x}\right) \,, \tag{2}$$

$$v = -\frac{k}{\mu}\left(\frac{\partial p}{\partial y} + \rho\, g\right) \,, \tag{3}$$

$$u\frac{\partial T}{\partial x} + v\frac{\partial T}{\partial y} = \alpha\frac{\partial^2 T}{\partial y^2} + \frac{D_m k_T}{C_s c_p}\frac{\partial^2 C}{\partial y^2} + \frac{q_w}{\rho\, c_p} - \frac{1}{\rho\, c_p}\frac{\partial q_r}{\partial y} \,, \tag{4}$$

$$u\frac{\partial C}{\partial x} + v\frac{\partial C}{\partial y} = D_m\frac{\partial^2 C}{\partial y^2} + \frac{D_m k_T}{T_m}\frac{\partial^2 T}{\partial y^2} \,, \tag{5}$$

$$\rho = \rho_\infty \Big[1 - \beta\,(T - T_\infty) - \beta^*\,(C - C_\infty)\Big]\,, \tag{6}$$

$$\frac{1}{\mu} = \frac{1}{\mu_\infty}\Big[1 + \delta\,(T - T_\infty)\Big]\,, \tag{7}$$

where u and v are the velocity components in the x- and y-directions, respectively, ρ and α denote the fluid density and the thermal diffusivity, p is the pressure, and g is the gravitational acceleration, T is the temperature of the fluid, k is the permeability of the porous medium, C is the concentration of the fluid and D_m is the mass diffusivity, c_p and C_s are the specific heat at constant pressure and concentration susceptibility, respectively. T_m is the mean fluid temperature, q_r is the radiative heat flux and q_w is the internal heat generation, k_T is the thermal-diffusion ratio, β is the thermal expansion coefficient and β^* is the concentration expansion coefficient, and δ is the constant. The subscript ∞ indicates condition at the ambient medium.

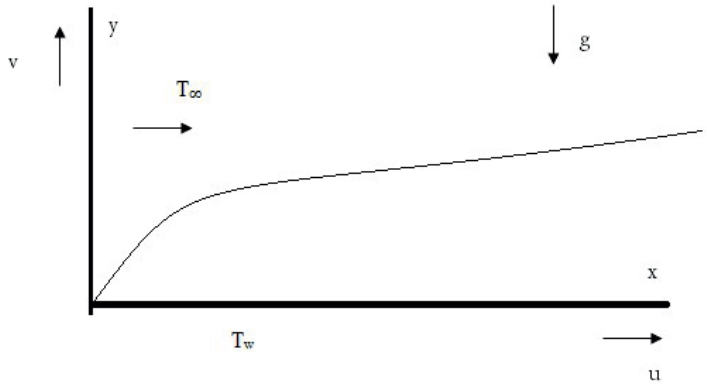

Figure 1: Physical model and coordinate system.

The dynamic viscosity of the fluid is assumed to be an inverse linear function of temperature and defined as $\mu = \dfrac{\mu_\infty}{(1 + \delta\,(T - T_\infty))}$, where δ is the thermal property of the fluid (Ling and Dybbs [27]).

The appropriate boundary conditions are as follows:

$$y = 0:\ v = 0\,, \qquad T = T_w\,, \qquad C = C_w\,, \tag{8}$$

$$y \to \infty:\ u \to 0\,, \qquad T \to T_\infty\,, \qquad C \to C_\infty\,. \tag{9}$$

3 Method of solution

The system of governing equations can be reduced by using the stream function $\psi(x,y)$ approach so that $u = \frac{\partial \psi}{\partial y}$ and $v = -\frac{\partial \psi}{\partial x}$. We introduce now the following similarity variables:

$$\psi = \alpha f \left(\mathrm{Ra}_x\right)^{\frac{1}{2}}, \qquad \theta = \frac{T - T_\infty}{T_w - T_\infty}, \qquad \text{and} \qquad \varphi = \frac{(C - C_\infty)}{(C_w - C_\infty)}, \tag{10}$$

where f is the dimensionless stream function. The local Rayleigh number is defined as

$$\mathrm{Ra}_x = \left[\frac{kg\beta\left(T_w - T_\infty\right)x}{\nu\alpha}\right]^{\frac{2}{3}}. \tag{11}$$

The internal heat generation which decays exponentially can be written as

$$q_w = \frac{\rho\, c_p\, \alpha\, \left(T_w - T_\infty\right)\, \mathrm{Ra}_x e^{-\eta}}{x^2}. \tag{12}$$

The optically thick radiation limit is considered in the present study. The gas is assumed to be an optically thick gas (i.e., intensive absorption) so that Rosseland approximation may be used for the radiative heat transfer, and the radiative heat flux term, q_r, is defined to be

$$q_r = -\frac{4\sigma_s}{3k_e}\frac{\partial T^4}{\partial y}, \tag{13}$$

where σ_s is the Stefan-Boltzmann constant and k_e is the mean absorption coefficient. The above expression that measures the radiative heat transfer is appropriate for two-dimensional boundary layer flow.

If the temperature differences within the flow are sufficiently small, then Eq. (13) can be linearized by expanding T^4 into the Taylor series about T_∞, which after neglecting higher order terms takes the form

$$T^4 \cong 4T_\infty^3 T - 3T_\infty^4. \tag{14}$$

Then the radiation term in Eq. (4) takes the form

$$\frac{\partial q_r}{\partial y} = \frac{16\sigma_s T_\infty^3}{3k_e}\frac{\partial^2 T}{\partial y^2}. \tag{15}$$

Substituting the expressions in (10)–(15) into the governing Eqs. (2)–(5), we obtain the following transformed equations:

$$f'' = \frac{f'\theta'}{\theta - \theta_c} - \frac{2}{3}\left(\frac{\theta - \theta_c}{\theta_c}\right)\left(\eta\theta' + \eta N\varphi'\right), \tag{16}$$

$$(1+R)\,\theta'' + \frac{1}{3} f\theta' + \mathrm{Pr}\,\mathrm{Du}\varphi'' + e^{-\eta} = 0\,, \tag{17}$$

$$\varphi'' + \mathrm{Sc}\,\mathrm{Sr}\theta'' + \frac{\mathrm{Le}}{3} f\varphi' = 0\,. \tag{18}$$

The boundary conditions (8) and (9) are transformed as follows:

$$f = 0\,, \qquad \theta = 1\,, \qquad \varphi = 1\,, \qquad \text{at} \;\; \eta = 0\,, \tag{19}$$

$$f' \to 0\,, \qquad \theta \to 0\,, \qquad \varphi \to 0\,, \qquad \text{as} \;\; \eta \to \infty\,, \tag{20}$$

where the prime and double prime symbols denote first and second order differentiation with respect to the variable η.

In the foregoing equations

$N = \dfrac{\beta^* (C_w - C_\infty)}{\beta (T_w - T_\infty)}$ is the buoyancy ratio of concentration to temperature,

$R = \dfrac{16\sigma_s T_\infty^3}{3k_e k}$ is the radiation parameter,

$\mathrm{Pr} = \dfrac{\nu}{\alpha}$ is the Prandtl number,

$\mathrm{Du} = \dfrac{D_m k_T (C_w - C_\infty)}{C_s c_p \nu (T_w - T_\infty)}$ is the Dufour number,

$\mathrm{Sc} = \dfrac{\nu}{D_m}$ is the Schmidt number,

$\mathrm{Sr} = \dfrac{D_m k_T (T_w - T_\infty)}{T_m \nu (C_w - C_\infty)}$ is the Soret number, and

$\mathrm{Le} = \dfrac{\alpha}{D_m}$ is the Lewis number.

In addition, $\theta_c = -\dfrac{1}{\delta (T_w - T_\infty)}$ is the parameter characterizing the influence of viscosity. For a given temperature difference, large values of θ_c implies either δ or $(T_w - T_\infty)$ is very small. In this case, the effect of variable viscosity can be neglected. The effect of variable viscosity is significant when θ_c is small. Since the viscosity decreases for liquids and increases for gases when temperature is increased, θ_c is negative for liquids and positive for gases. The notion of this parameter θ_c was first reported by Ling and Dybbs [31] in their paper of forced convection flow in porous media. The parameter N measures the relative importance of mass and thermal diffusion in the buoyancy-driven flow. It is obvious that N is zero for thermal-driven flow, infinite for mass driven flow, positive for aiding flow and negative for opposing flow.

The most remarkable characteristics of the problem are the rates of heat and mass transfer which are described by the local Nusselt number and Sherwood number, respectively, and are defined as follows:

$$\mathrm{Nu}_x = \frac{x}{\Delta T}\left(-\frac{\partial T}{\partial y}\right)_{y=0}, \quad \text{and} \quad \mathrm{Sh}_x = \frac{x}{\Delta C}\left(-\frac{\partial C}{\partial y}\right)_{y=0},$$

$$\frac{\mathrm{Nu}_x}{(\mathrm{Ra}_x)^{\frac{1}{2}}} = -\theta'(0) \ , \tag{21}$$

$$\frac{\mathrm{Sh}_x}{(\mathrm{Ra}_x)^{\frac{1}{2}}} = -\phi'(0) \ . \tag{22}$$

4 Results and discussion

Similarity transformation is employed to transform the governing equations into a set of coupled nonlinear differential equations. Equations (16)–(18) with the boundary conditions (19)–(20) were numerically solved by using the built in function bvp4c (boundary value probloem for ordinary differential equations) of the commercial software Matlab. This software uses the higher order finite difference code that implements a collocation formula (Shampine *et al.* [32]).

The effects on velocity, heat and mass transfer characteristics are investigated by varying the parameters variable viscosity, θ_c, which is an indicator of the variation of viscosity with temperature, radiation, R, Lewis number, Le, buoyancy ratio, N, Prandtl number, Pr, Dufour number, Du, Soret number, Sr and Schmidt number, Sc, in the presence of internal heat generation. Many commonly used fluids such as pure gases at room temperature ($0.67 \leq \mathrm{Pr} \leq 1$). Since the working fluid is optically thick gray gas, the corresponding Prandtl number at air in the ambient temperature is taken to be $\mathrm{Pr} = 0.73$.

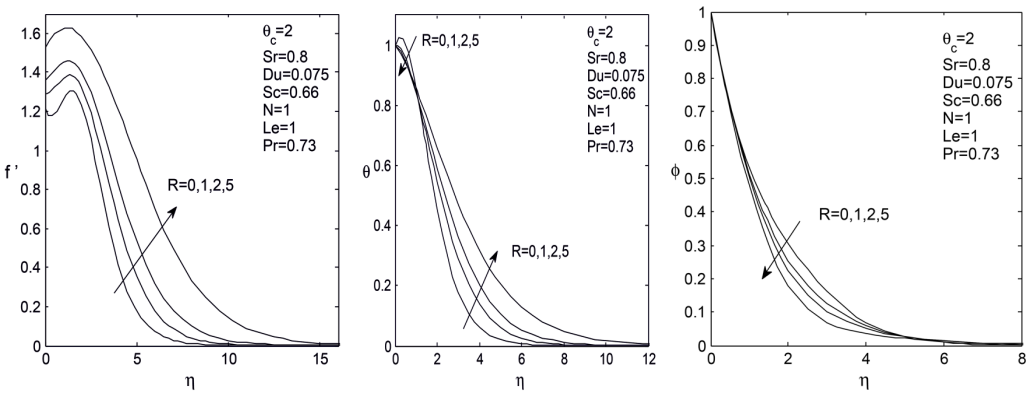

Figure 2: Effects of radiation parameter on dimensionless velocity (a), temperature (b), and concentration (c) profiles in the presence of internal heat generation.

The values of Schmidt number are chosen as Sc = 0.24, 0.62–0.66, and 0.78,

representing diffusing chemical species of most common interest in air like H_2, H_2O and NH_3, respectively. Three sets of values for the Dufour and Soret numbers such as Du = 0.3, Sr = 0.2; Du = 0.15, Sr = 0.4; and Du = 0.075, Sr = 0.8 are assumed. The choice of Dufour and Soret numbers is made so that their product is 0.06 according to their definition provided that the mean temperature is kept constant as well. The variable viscosity parameter is varied as $\theta_c = 2, 5$, and $\theta_c \to \infty$ to represent high viscosity, moderate viscosity, and ambient viscosity, respectively. The radiation parameter takes the values $R = 0$, 1, and 10 to denote, respectively, no radiation, moderate radiation and high radiation. The buoyancy ratio parameter presumes $N > 0$ for thermally assisting flow and $N < 0$ for opposing flow.

4.1 Velocity profiles

Figures 2(a), 3(a), 4(a), 5(a), and 6(a) illustrate the effects of various thermo-physical parameters on the fluid velocity profile. In all these figures of velocity profiles, the fluid velocity increases gradually near the plate and attains its peak value within the boundary layer. Further, the fluid velocity decreases to the free stream zero value, satisfying the boundary conditions. From Fig. 2(a) it can be noticed that thermal radiation parameter has remarkable effect on the velocity. The optically dense gray gas is accelerated rapidly near the surface of the plate and the momentum boundary-layer thickness increases due to the enhancement of radiation.

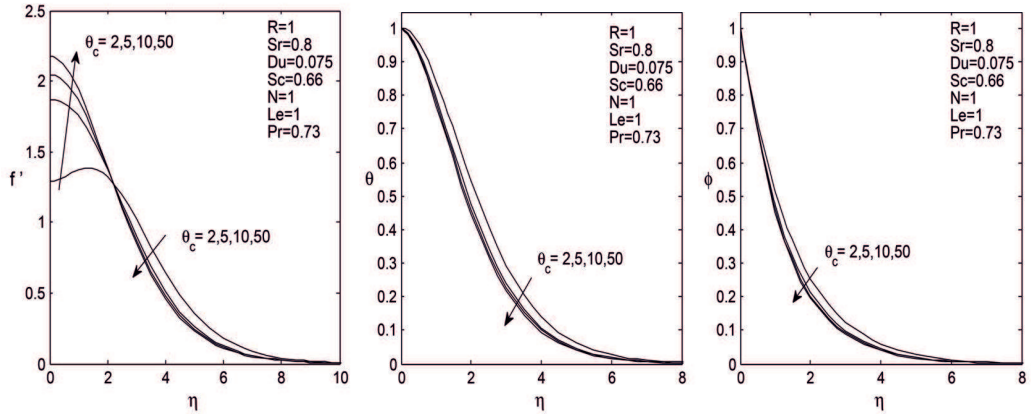

Figure 3: Effects of variable viscosity with internal heat generation on dimensionless velocity (a), temperature (b), and concentration profiles (c).

Figure 3(a) depicts that velocity increases near the plate and decreases away from the plate when the variable viscosity is varied from high viscosity ($\theta_c = 2$) to very low viscosity level ($\theta_c = 50$). Figure 4(a) shows that the velocity decreases slightly with the increase of Dufour number whereas it decreases with the decrease of Soret number. The effect of buoyancy ratio parameter, N, on the velocity profile is appreciable because the parameter N is explicitly present only in the momentum equation, which is illustrated in Fig. 5(a). The physical reason is that the buoyancy forces act like a pressure gradient which accelerates or decelerates the fluid within the boundary layer. The fluid acceleration is far better for assisting flow for the opposing flow though the velocity reaches peak value near the plate for both types of flows. It can be viewed in Fig. 6(a) that for both flows, the velocity profile is more elevated in the presence of internal heat generation. It can be physically understood that the internal heat generation results in an increase in the buoyancy forces which in turn induce more flow along the plate.

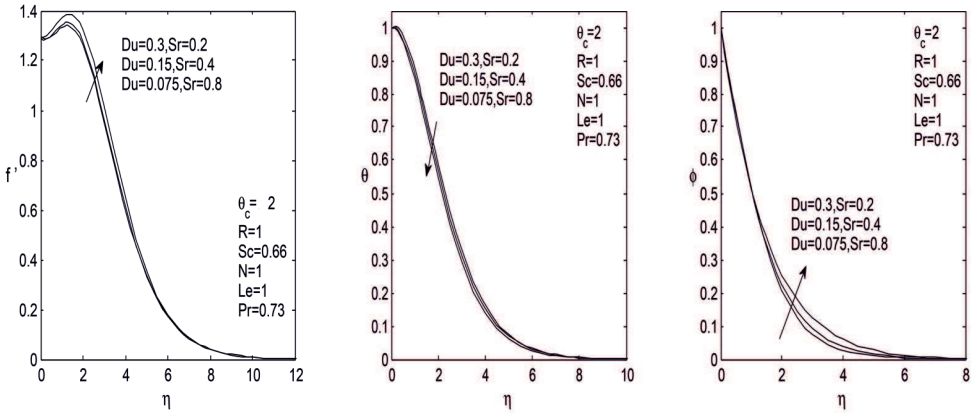

(a) (b) (c)

Figure 4: Dufour and Soret effects on dimensionless velocity (a), temperature (b), and concentration (c) profiles with internal heat generation.

4.2 Temperature profiles

The effects of various thermophysical parameters on the fluid temperature profile are demonstrated in Figs. 2(b), 3(b), 4(b), 5(b), and 6(b). These figures confirms that the fluid temperature is maximum at the plate surface and decreases exponentially to zero value far away from the plate satisfying the boundary conditions. From Fig. 2(b), it is noted that the thermal boundary layer thickness increases

with an increase in thermal radiation. The fluid temperature is slightly higher near the plate in the absence of radiation than in the presence of radiation, due to the internal heat generation. The results presented in Fig. 3(b) reveal quite clearly that viscosity parameter, θ_c, has a substantial effect on the temperature profile. Temperature of the fluid increases as the variable viscosity parameter decreases. The thermal boundary layer is developed better for high viscosity fluid than that of low viscosity fluid. From Fig. 4(b), it is evident that the temperature increases as Dufour number increases or Soret number decreases. The numerical results of Fig. 5(b) specifies that an increase in the buoyancy ratio parameter ($N > 0$) undoubtedly induces a strong reduction in the temperature of the fluid and consequently thinner thermal boundary layer occurs. In the opposing flow case ($N < 0$), when N varies from -0.3 to -0.9, the thermal boundary layer thickness increases. The thickness of the thermal boundary layer increases significantly when thermally opposing flow is considered.

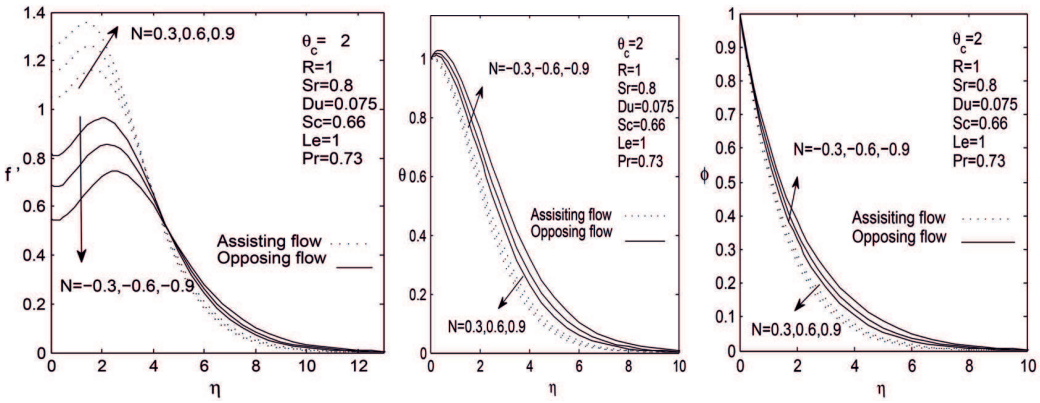

(a) (b) (c)

Figure 5: Effects of assisting and opposing flows with internal heat generation on dimensionless velocity (a), temperature (b), and concentration (c) profiles.

From Fig. 6(b) it is noted that the fluid temperature becomes maximum in the fluid layer adjacent to the wall rather than at the wall, when internal heat generation is present. In fact, the heat generation effect not only has the tendency to increase the fluid temperature but also increases the thermal boundary layer thickness. In the presence of heat generation, the temperature distribution is enhanced for assisting and opposing flows.

The negative sign in heat transfer rate in Tabs. 1 and 2 signifies the presence of internal heat generation for the considered isothermal plate. For low values of

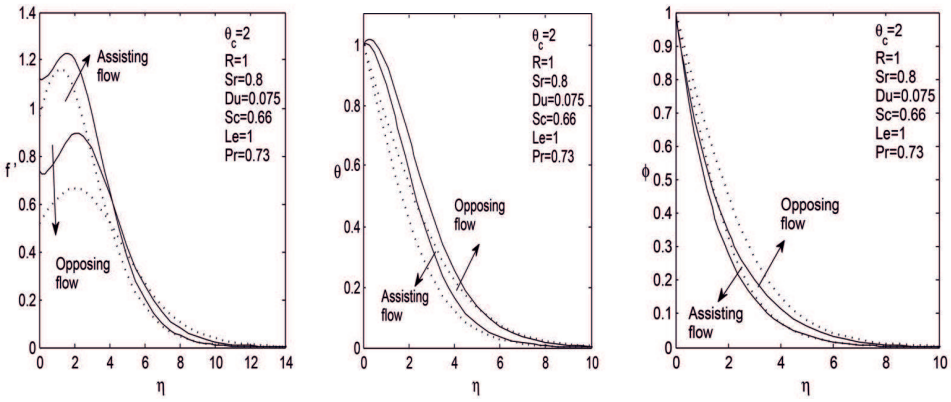

Figure 6: The profiles of velocity (a), temperature (b), and concentration (c) in the presence of internal heat generation (continuous line) and in the absence of internal heat generation (dotted line).

the radiation parameter, the values of local heat transfer rate are negative. This is an indication of the process in which the heated plate is cooled by the fluid. When fluid radiation increases, the value of Nusselt number becomes positive. This becomes good evidence that the temperature of the fluid is higher than that of the surface in assisting and opposing flow cases with internal heat generation. It is clearly observed from Tabs. 3 and 4 that the rate of local heat transfer decreases when fluid radiation is increased for both flow cases in the absence of internal heat generation.

In the case of assisting flow, the surface is cooled by the fluid with high viscosity when the internal heat generation is present. As far as the ambient viscosity is considered, the result is reversed. In other words, the fluid is hotter than the horizontal plate surface. This can be verified in Tab. 1. For all other cases, namely, assisting flow without internal heat generation and opposing flow with or without heat generation, the rate of heat transfer increases when fluid viscosity decreases towards constant viscosity. On increasing the Prandtl number, the heat transfer rate slightly decreases in the presence or absence of internal heat generation regardless of type of flows. Tables reveal the fact of these results.

In the presence of internal heat generation, the variations of Schmidt number from H_2 to H_20 and then to NH_3 for assisting flow case results in an insignificant increase in heat transfer rate. Further, in the opposing flow case, it is observed that heat transfer rate is decreased. On increasing Schmidt number, it is found that the heat transfer rate is increased for assisting flow and decreased for opposing

Table 1: The local Nusselt number and Sherwood number for thermally assisting flow ($N = 0.5$), $\mathrm{Du} = 0.15$ and $\mathrm{Sr} = 0.4$ in the presence of internal heat generation.

R	θ_c	Pr	Sc	Le	$-\theta'(0)$	$-\phi'(0)$
0	2	0.73	0.62	1	-0.2992	0.5656
1	2	0.73	0.62	1	-0.0647	0.5382
10	2	0.73	0.62	1	0.0900	0.5951
1	5	0.73	0.62	1	-0.0154	0.6068
1	∞	0.73	0.62	1	0.0112	0.6438
1	2	0.10	0.62	1	-0.0501	0.5336
1	2	1.00	0.62	1	-0.0711	0.5401
1	2	0.73	0.24	1	-0.0652	0.5081
1	2	0.73	0.78	1	-0.0645	0.5510
1	2	0.73	0.62	3	-0.0977	0.8736
1	2	0.73	0.62	7	-0.1250	1.2818

Table 2: The local Nusselt number and Sherwood number for thermally opposing flow ($N = -0.5$), $\mathrm{Du} = 0.15$ and $\mathrm{Sr} = 0.4$ in the presence of internal heat generation.

R	θ_c	Pr	Sc	Le	$-\theta'(0)$	$-\phi'(0)$
0	2	0.73	0.62	1	-0.4176	0.4979
1	2	0.73	0.62	1	-0.1224	0.4694
10	2	0.73	0.62	1	0.0813	0.5404
1	5	0.73	0.62	1	-0.0778	0.5280
1	∞	0.73	0.62	1	-0.0539	0.5595
1	2	0.10	0.62	1	-0.1112	0.4641
1	2	1.00	0.62	1	-0.1274	0.4717
1	2	0.73	0.24	1	-0.1178	0.4367
1	2	0.73	0.78	1	-0.1244	0.4834
1	2	0.73	0.62	3	-0.1176	0.7980
1	2	0.73	0.62	7	-0.1316	1.2010

Table 3: The local Nusselt number and Sherwood number for thermally assisting flow ($N = 0.5$), Du = 0.15 and Sr = 0.4 in the absence of internal heat generation.

R	θ_c	Pr	Sc	Le	$-\theta'(0)$	$-\phi'(0)$
0	2	0.73	0.62	1	0.4147	0.3815
1	2	0.73	0.62	1	0.3114	0.4386
10	2	0.73	0.62	1	0.1662	0.5738
1	5	0.73	0.62	1	0.3437	0.4928
1	∞	0.73	0.62	1	0.3623	0.5236
1	2	0.10	0.62	1	0.3217	0.4339
1	2	1.00	0.62	1	0.3068	0.4406
1	2	0.73	0.24	1	0.3081	0.4565
1	2	0.73	0.78	1	0.3127	0.4309
1	2	0.73	0.62	3	0.2788	0.7639
1	2	0.73	0.62	7	0.2522	1.1520

Table 4: The local Nusselt number and Sherwood number for thermally opposing flow ($N = -0.5$), Du = 0.15 and Sr = 0.4 in the absence of internal heat generation.

R	θ_c	Pr	Sc	Le	$-\theta'(0)$	$-\phi'(0)$
0	2	0.73	0.62	1	0.2749	0.2523
1	2	0.73	0.62	1	0.2474	0.3428
10	2	0.73	0.62	1	0.1572	0.5156
1	5	0.73	0.62	1	0.2735	0.3859
1	∞	0.73	0.62	1	0.2885	0.4105
1	2	0.10	0.62	1	0.2528	0.3363
1	2	1.00	0.62	1	0.2449	0.3455
1	2	0.73	0.24	1	0.2502	0.3629
1	2	0.73	0.78	1	0.2461	0.3343
1	2	0.73	0.62	3	0.2559	0.6664
1	2	0.73	0.62	7	0.2441	1.0508

flow in the absence of internal heat generation. When Lewis number is increased, the rate of heat transfer decreases for assisting flow without the consideration of presence or absence of internal heat generation. In the opposing flow pattern, an increase in heat transfer rate is observed for Le = 1–3, whereas it shows that heat transfer rate is decreased for Le = 3–7.

4.3 Concentration profiles

The effects of various thermophysical parameters on the fluid concentration profile are depicted in Figs. 2(c), 3(c), 4(c), 5(c), and 6(c). It can be noted from Fig. 2(c) that the concentration boundary layer thickness decreases away from the plate surface with an increase in the thermal radiation. Moreover, concentration of the fluid is decreased as fluid radiation increases. Figure 3(c) confirms that the fluid concentration profile increases while the variable viscosity parameter, θ_c, is decreased. It is evident that the concentration decreases for an increase in Dufour number while Soret number is decreased. This is shown in Fig. 4(c). The results indicated in Fig. 5(c) reveals that an increase in the buoyancy ratio parameter ($N > 0$) leads to a strong reduction in the concentration of the fluid. In the opposing flow case ($N < 0$), the concentration boundary layer thickness increases on varying N from -0.3 to -0.9. Obviously, Fig. 6(c) explicates that the internal heat generation significantly decreases the concentration boundary layer thickness for both flow cases.

For the presence or absence of internal heat generation and for both types of flow, it can be understood that the rate of mass transfer increases with the increase in the radiation parameter, R. From high viscous fluid state to constant fluid viscosity state, the mass transfer rate significantly increases. When Prandtl number increases, an increase is obtained in the local Sherwood number. On increasing Lewis number, a significant increase is observed in the mass transfer rate. These can be confirmed from the tabulated numerical results.

Under both types of flow, the variation in Schmidt number from H_2 to H_20 and then to NH_3, the mass transfer rate increases in the presence of internal heat generation. On the contrary, mass transfer rate decreases for the absence of internal heat generation.

5 Conclusions

In presented study, the effects of radiation, variable viscosity, Dufour and Soret effects on heat and mass transfer characteristics over a horizontal surface in the presence of internal heat generation are numerically investigated. A flux model has been employed to simulate thermal radiation effects, valid for optically thick gases. The governing boundary layer equations for the present problem are transformed into nonlinear ordinary differential equations by using similarity transformations. Commercial boundary value problem solver for ordinary differential equations (Matlab bvp4c) is used to compute the numerical results. The obtained solutions for the variations of the controlling parameters are represented

graphically. The drawn conclusions for the present work after a thorough observation are summarized as follows:

1. Presence of internal heat generation elevates the velocity profile better and significantly decreases the concentration boundary layer thickness regardless of the types of flows. In addition, the optically dense gray gas is accelerated rapidly near the surface of the plate.

2. The thickness of the thermal boundary layer increases with thermally opposing flows than with thermally assisting flows. For assisting flow, the surface is cooled by the fluid with high viscosity when the internal heat generation is present.

3. An increase in the assisting flow parameter leads to a strong reduction in the temperature and concentration profiles of the fluid in the presence of internal heat generation.

4. When fluid radiation increases, the temperature of the fluid is higher than that of the surface and the concentration boundary layer thickness decreases away from the surface for both types of flow in the presence of internal heat generation.

5. On increasing Schmidt number, the heat transfer rate is increased for assisting flow and decreased for opposing flow in the absence of internal heat generation.

Received 7 July 2015 and in revised form 20 June 2017

References

[1] Ingham D.B., Pop. I.: *Transport Phenomena in Porous Media III.* Elsevier, Oxford 2005.

[2] Nield D.A., Bejan. A.: *Convection in Porous Media*, 3rd Edn. Springer, New York 2006.

[3] Vafai K.: *Handbook of Porous Media,* Taylor and Francis, New York 2005.

[4] Cheng P., Minkowycz W.J.: *Free convection about a vertical plate embedded in a porous medium with application to heat transfer from a dike.* J. Geophysical Res. **82**(1977), 14, 2040–2044.

[5] Lai F.C., Kulacki. F.A.: *The effect of variable viscosity on convection heat transfer along a vertical surface in a saturated porous medium.* Int. J. Heat Mass Tran. **33**(1990), 5, 1028–1031.

[6] Mehrizi A. A., Vazifeshenas Y, Domairry G.: *New analysis of natural convection boundary layer flow on a horizontal plate with variable wall temperature.* J. Theor. App. Mech-Pol. **50**(2012), 1001–1010.

[7] Henclik S.: *Mathematical model and numerical computations of transient pipe flows with fluid-structure interaction.* Trans. Ins. Fluid-Flow Mach. **122**(2010), 77–94.

[8] Eckert E.R.G., Drake R.M. : *Analysis of Heat and Mass Transfer.* McGraw-Hill, New York 1972.

[9] Badur J., Karcz M., Lemański M., Nastałek L.: *Foundations of the Navier-Stokes boundary conditions in fluid mechanics.* Trans. Inst. Fluid-Flow Mach. **123**(2011), 3–55.

[10] Anghel M., Takhar H.S., Pop I.: *Dufour and Soret effects on free convection boundary layer over a vertical surface embedded in a porous medium.* Studia Universitatis Babes-Bolyai Mathematica. XLV(2000), 11–22.

[11] Lakshmi Narayana P.A., Murthy P.V.S.N.: *Soret and Dufour effects on free convection heat and mass transfer from a horizontal flat plate in a Darcy porous medium.* ASME J. Heat Transfer **130**(2008), 10, 104504-1–104504-5.

[12] El-Arabawy H.A.M. : *Soret and Dufour effects on natural convection flow past a vertical surface in a porous medium with variable surface temperature.* J. Math Stat. **5**(2009), 3, 190–198.

[13] Tai B.C., Char M.I.: *Soret and Dufour effects on free convection flow of non-Newtonian fluids along a vertical plate embedded in a porous medium with thermal radiation.* Int. Commun. Heat Mass **37**(2010), 480–483.

[14] Crepeau J.C., Clarksean R.: *Similarity solutions of natural convection with internal heat generation.* J. Heat Trans. **119**(1997), 1, 183–185.

[15] Postelnicu A., Pop I.: *Similarity solutions of free convection boundary layers over vertical and horizontal surfaces in porous media with internal heat generation.* Int. Commun. Heat Mass **26**(1999), 8, 1183–1191.

[16] Alam M.S., Rahman M.M., Samad M.A.: *Numerical study of the combined free-forced convection and Mass transfer flow past a vertical porous plate in a porous medium with heat generation and thermal diffusion.* Nonlinear Anal-Model. **11**(2006), 4, 331–343.

[17] Sharma P.R.: *Effects of varying viscosity and thermal conductivity on steady MHD free convective flow and heat transfer along an isothermal plate with internal heat generation.* Int. J Numerical Method 19 (2009), 1, 78–92.

[18] Makinde O.D.: *Similarity solution for natural convection from a moving vertical plate with internal heat generation and a convective boundary condition.* Therm. Sci. Int. Sci J. **15**(2011), Suppl. 1, 137–143.

[19] Raptis A.: *Radiation and free convection flow through a porous medium.* Commun. Heat Mass **25**(1998), 2, 289–295.

[20] Hossain M.A., Takhar H.S.: *Thermal radiation effects on natural convection flow over an isothermal horizontal plate.* Heat Mass Transfer **35**(1999), 4, 321–326.

[21] Hossain M.A., Khanafer K., Vafai K.: *The effect of radiation on free convection flow of fluid with variable viscosity from a porous vertical plate.* Int. J. Therm. Sci. **40**(2001), 2, 115–124.

[22] Magyari E., Pantokratoras A. : *Note on the effect of thermal radiation in the linearized Rosseland approximation on the heat transfer characteristics of various boundary layer flows*. Int. Commun. Heat Mass **38**(2011), 554–556.

[23] Siddiqa S., Hossain M.A., Saha S.C.: *The effect of thermal radiation on the natural convection boundary layer flow over a wavy horizontal surface*. Int. J. Therm. Sci. **84**(2014), 143-150.

[24] Rup K., Dróżdż A.: *The effect of reduced heat transfer in a micropolar fluid in natural convection.* Arch. Thermodyn **34**(2013), 3, 45–59.

[25] Roszko A., Fornalik-Wajs E.: *The heat transfer and flow structure analyses of low concentration copper nanofluids in a strong magnetic field*. Trans. Inst. Fluid-Flow Mach. **128**(2015), 29–42.

[26] Lai F.C., Kulacki F.A.: *Coupled heat and mass transfer by natural convection from vertical surfaces in porous media*. Int. J. Heat Mass Tran. **34**(1991), 4-5, 1189–1994.

[27] Kumari M.: *Variable viscosity effects on free and mixed convection boundary layer flow from a horizontal surface in a saturated porous medium-variable heat flux.* Mech. Res. Commun. **28**(2001), 3, 339–348.

[28] Kannan, T., Moorthy M.B.K.: *Effects of variable viscosity on power-law fluids over a permeable moving surface with slip velocity in the presence of heat generation and suction*. J. Appl. Fluid Mech. **9**(2016), 6, 2791–2801.

[29] Makinde O.D.: *Effect of variable viscosity on thermal boundary layer over a permeable flat plate with radiation and a convective surface boundary condition.* J. Mech. Sci. Technol. **26**(2012), 5, 1615–1622.

[30] Cieśliński J.T., Ronewicz K., Smoleń S.: *Measurement of temperature-dependent viscosity and thermal conductivity of alumina and titania thermal oil nanofluids.* Arch. Thermodyn. **36**(2015), 4, 35–47.

[31] Ling J.X., Dybbs A.: *Forced convection over a flat plate submersed in a porous medium: variable viscosity case*. In: Proc. ASME 87-WA/HT-23, New York 1987.

[32] Shampine L.F., Kierzenka J., Reichelt M.W. : *Solving boundary value problems for ordinary differential equations in MATLAB with bvp4c*. http://www.mathworks.com/bvp_tutorial 2003